RESEARCH ARTICLE | FEBRUARY 26 2015

Induction-detection electron spin resonance with spin sensitivity of a few tens of spins FREE

Yaron Artzi; Ygal Twig; Aharon Blank

Appl. Phys. Lett. 106, 084104 (2015)
https://doi.org/10.1063/1.4913806

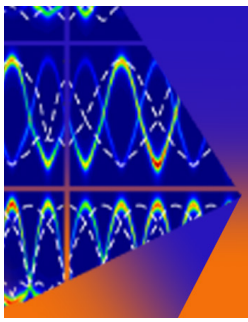

Induction-detection electron spin resonance with spin sensitivity of a few tens of spins

Yaron Artzi, Ygal Twig, and Aharon Blank
Schulich Faculty of Chemistry Technion—Israel Institute of Technology, Haifa 32000, Israel

(Received 26 January 2015; accepted 17 February 2015; published online 26 February 2015)

Electron spin resonance (ESR) is a spectroscopic method that addresses electrons in paramagnetic materials directly through their spin properties. ESR has many applications, ranging from semiconductor characterization to structural biology and even quantum computing. Although it is very powerful and informative, ESR traditionally suffers from low sensitivity, requiring many millions of spins to get a measureable signal with commercial systems using the Faraday induction-detection principle. In view of this disadvantage, significant efforts were made recently to develop alternative detection schemes based, for example, on force, optical, or electrical detection of spins, all of which can reach single electron spin sensitivity. This sensitivity, however, comes at the price of limited applicability and usefulness with regard to real scientific and technological issues facing modern ESR which are currently dealt with conventional induction-detection ESR on a daily basis. Here, we present the most sensitive experimental *induction-detection* ESR setup and results ever recorded that can detect the signal from just a few tens of spins. They were achieved thanks to the development of an ultra-miniature micrometer-sized microwave resonator that was operated at ∼34 GHz at cryogenic temperatures in conjunction with a unique cryogenically cooled low noise amplifier. The test sample used was isotopically enriched phosphorus-doped silicon, which is of significant relevance to spin-based quantum computing. The sensitivity was experimentally verified with the aid of a unique high-resolution ESR imaging approach. These results represent a paradigm shift with respect to the capabilities and possible applications of induction-detection-based ESR spectroscopy and imaging. © *2015 AIP Publishing LLC*.
[http://dx.doi.org/10.1063/1.4913806]

Magnetic resonance (MR) is one of the most powerful methods of scientific observation. MR is concerned mainly with methodologies for observing nuclear spins (Nuclear Magnetic Resonance, NMR) and electron spins (Electron Spin Resonance, ESR). It has a wide array of applications, ranging from the determination of chemical structure and molecular dynamics to medical imaging and quantum computing. Despite the success of MR methodologies, their application is typically limited by sensitivity (the number of spins that can be detected) and by their coarse spatial resolution. For example, even in ESR, which is inherently more sensitive than NMR, in the most favorable case of a sample having a narrow ESR spectrum, commercial ESR systems require at least 10^9 spins to achieve a measurable signal during 1 s of acquisition.[1] Such limited sensitivity also restricts the available imaging resolution of heterogeneous samples. Therefore, while the laws of physics do not set a limit on the spatial resolution of ESR (at least up to the atomic length scale), in practice, as its voxel size decreases, the image contains fewer and fewer spins and thus quickly comes up against the sensitivity limitation barrier. For example, commercial systems, e.g., from Bruker, have ∼25–μm resolution. Overcoming these two barriers of limited sensitivity and spatial resolution will pave the way for transformative developments in the experimental sciences.

While commercial systems have limited sensitivity and imaging resolution, recent work on "home-made" systems has pushed further the boundaries of induction-detection ESR sensitivity and imaging resolution, reaching a sensitivity of $\sim 3.2 \times 10^4$ spins/$\sqrt{\text{Hz}}$ (i.e., with 1 s of acquisition time),[2] and a spatial resolution (limited by the sensitivity) that is better than ∼500 nm.[2,3] Nevertheless, these results are still far from the ultimate sensitivity limit of a single electron spin, and the corresponding spatial resolution is still too coarse-grained for most modern scientific and technological applications.

The abovementioned values for sensitivity and resolution refer to ESR systems that employ *induction-detection*, i.e., they make use of Faraday's law for the detection of ESR signals by means of a pick-up coil or a microwave (MW) resonator. Induction-detection is the basic principle underlying all commercial state-of-the-art ESR systems: it allows the acquisition of high-resolution spectroscopic data using complex pulse sequences; it facilitates the use of efficient imaging methodologies (meaning that signals are acquired and averaged in *a parallel fashion* from the entire sample); and it features convenient sample handling. Whereas, our work is focused on induction-detection ESR, other groups have looked into alternative detection methods in an attempt to increase sensitivity and resolution. One of the best-known alternative approaches is magnetic resonance force microscopy,[4] which detects the force inflicted by the spins on a sharp magnetic tip and has demonstrated a single-electron-spin detection capability and 2D imaging with nanoscale resolution.[5] Another method is Scanning Tunneling Microscopy ESR (STM-ESR),[6] which combines the high spatial resolution of STM with the electronic spin sensitivity of ESR and can measure the signal from a single spin with

subnanometer 2D resolution. Other methods of possible relevance are spin-polarized STM,[7] electrically detected magnetic resonance,[8,9] and spin detection via diamond nitrogen-vacancy (NV) centers.[10]

While these and other related techniques are very impressive, *they all have inherent limitations that result in limited applicability*. These limitations refer to the fact that said techniques [a] are highly specific to particular samples and experimental conditions, [b] require complex procedures for sample preparation, [c] lack advanced spectroscopic capabilities, [d] operate efficiently only on or very close to the surface (a few nanometers), and [e] use mechanical movement to scan and image samples in a sequential manner. *Thus, in many ways, they can be considered only as complementary to induction-detection schemes*. As a result, the vast majority of useful scientific magnetic resonance data can currently be collected *only* using traditional induction-detection methods; and it seems likely that this trend will continue in the foreseeable future. Thus, every small (and certainly large) improvement in induction-detection capabilities could immediately be translated into better scientific data and a wider scope of applications, which is at the heart of the issues presented in this manuscript.

The key to our previous improvements in high-sensitivity ESR was the introduction of a unique type of MW resonator, known as an ultra-miniature surface loop-gap microresonator.[11,12] Such type of resonator, with a typical size of $\sim$20 μm, was operated in our previous efforts at a frequency of $\sim$15 GHz and cryogenic temperatures, in conjunction with a cryogenically cooled ultra-low-noise amplifier, and showed a capability to measure less than 1000 electron spins in $\sim$1 h of averaging time.[2] In principle, the smaller the resonator that collects the ESR signal, the better its absolute spin sensitivity.[13,14] Furthermore, the higher the static field employed (larger microwave frequency), the more sensitive the setup could be. Our previous efforts to use even smaller resonators, but still at $\sim$15 GHz, fell short due to the difficulty of efficient coupling of the MW energy (with a wavelength of $\sim$20 mm) into and out of such small micron-sized structures. Here, we significantly improve upon our previous attempts by moving to a larger static field corresponding to MW frequency of $\sim$34 GHz (wavelength of $\sim$9 mm). This enables us to couple the energy to a much smaller resonator, with typical dimensions of $\sim$2 μm. The combination of a smaller resonator and large static field, together with the use of a unique cryogenically cooled preamplifier to limit noise contribution, enabled us to obtain spin sensitivity of just $\sim$6697 spins/$\sqrt{\text{Hz}}$. Such capability is of significance to a variety of scientific and technological fields. For example, it can enable structural biology research based on small amounts of proteins and micron-sized single crystals; it can be used to provide 3D noninvasive mapping of semiconductor devices; and it may be used as a foundation for spin-based quantum computers. Below we provide the experimental results that actually confirm the capability to measure such small magnetization using induction detection.

The ESR measurements were carried out using the "home-made" pulsed imaging system described in details in Ref. 3. Briefly, the system includes a wideband microwave spectrometer that covers the 6–18 and 32–37 GHz range (Q-band), a microimaging probe head, gradient current drivers for spatial encoding of the spins, and control software. The system is capable of acquiring high-resolution four-dimensional ESR images (3 spatial axes and 1 spectral axis). For the purposes of the present work, we developed a unique cryogenic microimaging probe head that is at the core of the system and facilitates its high sensitivity. Figure 1 presents the design of the Q-band cryogenic microimaging probe

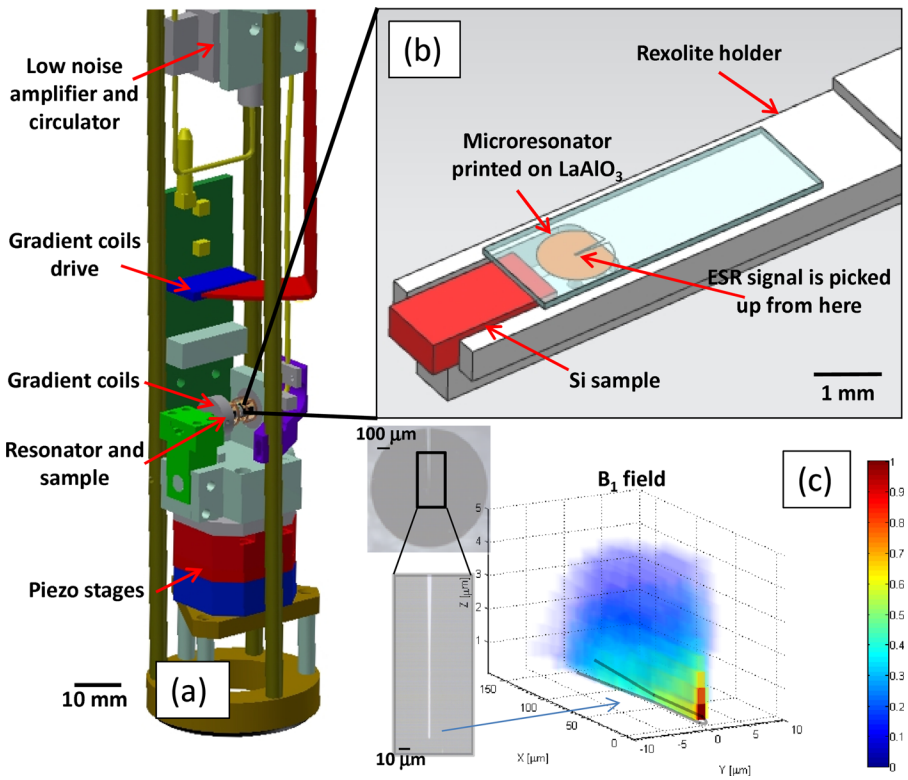

FIG. 1. The ultra-high-sensitivity Q-band cryogenic microimaging probe head. (a) The main part of the probe head that is cooled at the cryostat, featuring its major components. (b) The microresonator with the Si sample displaced, for better clarity of the graphics. (c) Optical image of the microresonator and a 3D plot showing the normalized distribution of the microwave magnetic field (B_1) at the center of the resonator.

head and the miniature resonator used in this work. It resembles our previous cryogenic imaging probe, which operates at a frequency of ∼12–18 GHz.[2] The main difference between the present configuration and the older design is the use of a miniature surface loop-gap resonator that now operates at ∼34 GHz and has an inner width of only 2 μm, with an overall effective volume[15] of just 27 pl. Details of the resonator, which is made by photolithography with copper deposited on a $LaAlO_3$ single-crystal substrate, are provided in Fig. 1(c). In addition, we employed a unique cryogenically cooled low noise preamplifier[16] with noise temperature of ∼7 K. Another critical component that had to be replaced in the old design is the circulator. While there is no commercially available circulator for Q-band that is specifically made to operate at cryogenic temperatures and has magnetic shielding, it turns out that model D3C2640 from DiTom Microwave Inc., exhibited adequate performances, even at low temperatures and under a static field of ∼0.3 T (we provided partial shielding from outside the cryostat).

The sample used in the present experiments is made of a thin 10-μm layer of phosphorus-doped ^{28}Si (^{28}Si:P) with 10^{16} P atoms per cubic centimeter with ^{28}Si purity of more than 99.9%, placed on a high-resistivity p-type silicon substrate.[17] At a temperature of 10 K, its measured T_1, T_2, and T_2* values were found to be 1 ms, 260 μs, and 0.8 μs, respectively.

In order to quantify the sensitivity of the setup described above, the experiment included two simple measurements: acquiring the signal of the ^{28}Si:P sample when the static field is exactly on-resonance; and then measuring the noise under the exact same experimental conditions but well off-resonance with respect to the static field. The results of these two measurements for an averaging time of 1 s are shown in Fig. 2, and the experimental details are provided in the caption. The ESR signal over a bandwidth of 1 MHz divided by the standard deviation of the noise (around the spectral position of the signal) was found to be ∼291.

The only part missing in this ESR sensitivity jigsaw puzzle is the provision of reliable information regarding the number of spins actually measured by our microresonator. Inspection of the experimental setup and the sample-resonator layout (Fig. 1(b)) reveals that the sample is relatively very large (and therefore contains a relatively large number of spins). However, the actual number of spins that are being excited and detected by the resonator is much smaller due to the confined microwave magnetic field (B_1) mode of the resonator (Fig. 1(c)). Based on the calculated three-dimensional B_1 field of the resonator, it is possible to numerically calculate the expected signal from any given part of the sample.[18] Figure 3(a) shows the result of such calculation, assuming a flip angle of 570° for the first pulse in the CPMG sequence (instead of the nominal 90°) at the point of the strongest B_1, just at the center of the resonator. This flip angle was chosen based on the calculated $B_1/\sqrt{W}$ of the resonator (which is 1290 $G/\sqrt{W}$), and the good correspondence it generates between the calculated and measured ESR signal distribution map (see below, Fig. 3(b)). (When employing other power levels, different images appeared due

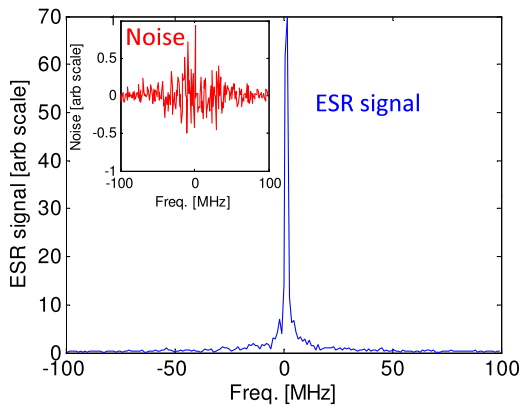

FIG. 2. ESR signal and noise in the spectral domain for the ^{28}Si:P sample at 10 K, around a center frequency of 34.1 GHz using a MW peak power of 0.2 mW. For signal acquisition, we employed a Carr-Purcell-Meiboom-Gill (CPMG) pulse sequence with a repetition rate of 600 Hz, $\pi/2$ pulse length of 30 ns, $\pi/2$-π pulse separation, $\tau = 1.2$ μs, and a data acquisition window of 1 μs. Data are averaged from shot to shot and also along each of the 160-π-pulse CPMG echo trains, resulting in overall $600 \times 160 = 96\,000$ averages in 1 s.

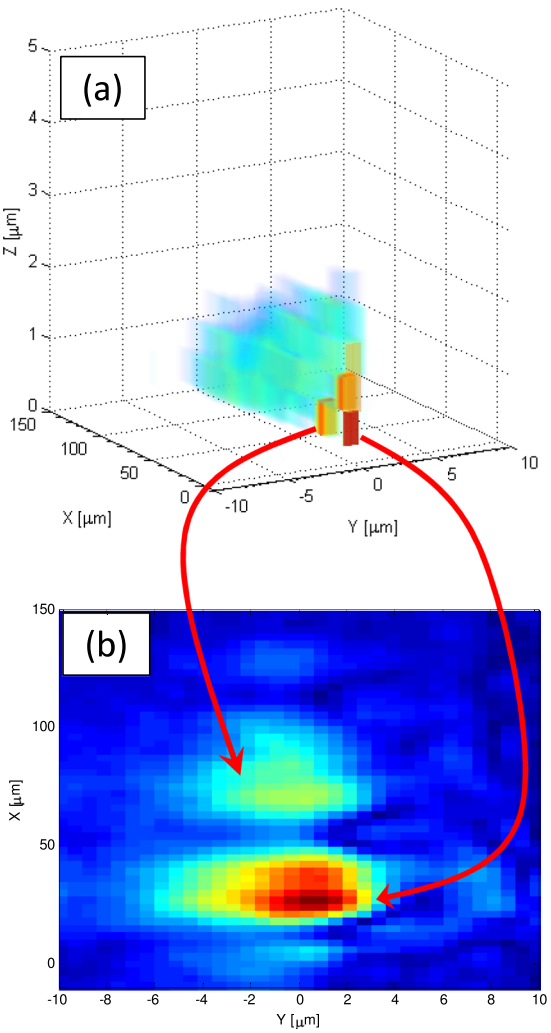

FIG. 3. (a) Calculated 3D ESR signal distribution from positions in the sample near the center of the resonator, based on the 3D B_1 field distribution (shown in Fig. 1(c)). (b) Measured 2D ESR signal distribution employing ESR micro-imaging technique, using the imaging pulse sequence described in Ref. 24 and the same CPMG sequence parameters as in Fig. 2. The red arrows show the correspondence between the predicted and measured signal distribution that is modulated due to B_1 variation when moving away from the center of the resonator.

to the different flip angles in various parts of the sample.) Based on this calculation of the 3D ESR signal map, it was found that most of the signal comes from a volume of ~100 μm^3, which corresponds to the measurement of ~1 000 000 spins. Support for this claim comes from our microimaging experiments, in which we make use of the high-resolution pulsed ESR imaging capability that is integral to our cryogenic imaging probe head and provides an actual image of the parts in the sample from which the signal is collected. This two-dimensional imaging result, provided in Fig. 3(b), shows good qualitative resemblance to the numerical electromagnetic simulations, but the corresponding volume from which the signal is collected is found here to be somewhat larger than the calculated results, namely, $\sim 6 \times 22 \times 1.5$ μm (the extension along the z-axis, which is not imaged in this case, is conservatively assumed to be 1.5 μm, due to the fast decay of the B_1 field out of the resonator plane; see Fig. 1(c)). This means that we measure a signal from $\sim 1.95 \times 10^6$ spins.

From now on, we will assume that the number of spins in the sample that are in our measurement zone is indeed 1.95×10^6, although we believe that this slightly overestimates the actual number of spins since our image may be prone to some smearing artifacts due to possible vibrations when operating our pulsed field gradients at a high field of ~1.2 T. Let us therefore calculate, on the basis of these numbers, the sensitivity of the setup in terms of the smallest magnetization (magnetic moment) it can actually detect by induction detection. The 1.95×10^6 spins provided us with a signal-to-noise-ratio (SNR) of ~291 in 1 s of acquisition time or ~6697 spins/$\sqrt{}$Hz. The maximum available (reasonable) measurement time of our setup is ~12 h, and averaging over this time period provides an additional factor of $\sqrt{}(3600 \times 12) = 208$ to the sensitivity (this has been verified in many of our past experiments, when we imaged and acquired data for such long periods of times with a corresponding increase in sensitivity[2,3]). *This brings the minimum number of detectable spins in our setup to 6697/208 ~ 32.*

While the *total* number of spins required to provide a measurable signal in our setup is ~32, it is worthwhile to estimate the actual net number of spins that contribute to the signal. This can be calculated based on the known Boltzmann population distribution of the electron spins in their Zeeman levels (note that the statistical spin polarization is averaged out in multiple averaging acquisition schemes). At 10 K and a field of ~1.2 T, only 8% of the spins actually contribute to the signal, which brings us to a net magnetization originating from just $0.08 \times 32 = 2.56$ spins. Furthermore, in the test sample of phosphorus-doped Si there are two spectral lines (due to the phosphorus nuclei's hyperfine interaction[19]), only one of which was measured by us, meaning a further decrease by a factor of 2 of the actual magnitude of the spins' magnetization measured. Therefore, when considering the Boltzmann population factor our results correspond to achieving the detection sensitivity of the *net magnetization* originating from just a single spin (~1.3 spins, to be exact) in an overnight experiment.

In conclusion, an experimental setup is described that enables the detection of a few tens of spins, which correspond to the *net* magnetization of approximately a single electron spin using a classical induction-detection ESR experiment. This is ~4–5 orders of magnitude better than the best commercial systems and more than one order of magnitude better than previous experimental achievements. In many spin systems, one can incorporate pre-polarization schemes that can fully polarize the spins' population and thus eliminate the Boltzmann factor.[20,21] This may ultimately lead to a capability to detect samples whose *total* number of spin is just one. Single-spin ESR with induction detection constitutes a paradigm shift in a field that traditionally relied on large numbers of spins, a condition that significantly limited its strength. Our results are thus of immediate importance to the field of spin-based quantum computing, which heavily relies on an ability to detect single spins. The spin system we measured is also very popular in this field and the fact that we relate to *net* polarized magnetization as a sensitivity ruler goes along well with the requirement and the availability of techniques to polarize the electrons as a requisite for any quantum computing algorithm.[22,23] An additional benefit of the presented induction-detection setup is that it does not require the measurement apparatus to be in nanometer proximity to the spin system as in probe-based methods (but rather at a distance of ~1 μm). Furthermore, it can be coupled with high-resolution MRI-like imaging methods for parallel spatially selective addressing and manipulation of spins, which brings all the power of conventional MR to the nanoscale world. This parallel nature of induction detection-based imaging assures that the averaging time that enables the detection of a single spin would be the same also for measuring many spins that must be individually addressed and/or imaged. Near-future improvements employing even smaller surface microresonators at a field of ~3.4 T (95 GHz), and possibly replacing the copper layer with a superconducting one with high quality factor can further increase the sensitivity of the approach, which may then be able to cope with the ultra-high-sensitivity spin detection of additional types of samples, not only those based on ^{28}Si:P spins.

This work was partially supported by Grant No. 310/13 from the Israel Science Foundation (ISF), and Grant No. FA9550-13-1-0207 from the Air Force Office of Scientific Research (AFOSR). We greatly acknowledge Dr. Wayne D. Hutchison (The University of New South Wales, Australia) for supplying us with the ^{28}Si:P sample.

[1]D. Schmalbein, G. G. Maresch, A. Kamlowski, and P. Hofer, Appl. Magn. Reson. **16**(2), 185 (1999).
[2]A. Blank, E. Dikarov, R. Shklyar, and Y. Twig, Phys. Lett. A **377**(31–33), 1937 (2013).
[3]L. Shtirberg, Y. Twig, E. Dikarov, R. Halevy, M. Levit, and A. Blank, Rev. Sci. Instrum. **82**(4), 043708 (2011).
[4]D. Rugar, R. Budakian, H. J. Mamin, and B. W. Chui, Nature **430**(6997), 329 (2004).
[5]C. L. Degen, M. Poggio, H. J. Mamin, C. T. Rettner, and D. Rugar, Proc. Natl. Acad. Sci. U. S. A. **106**(5), 1313 (2009).
[6]C. Durkan and M. E. Welland, Appl. Phys. Lett. **80**(3), 458 (2002).
[7]F. Meier, L. H. Zhou, J. Wiebe, and R. Wiesendanger, Science **320**(5872), 82 (2008).
[8]W. Harneit, C. Boehme, S. Schaefer, K. Huebener, K. Fostiropoulos, and K. Lips, Phys. Rev. Lett. **98**(21), 216601 (2007).
[9]M. Xiao, I. Martin, E. Yablonovitch, and H. W. Jiang, Nature **430**(6998), 435 (2004).

[10]M. S. Grinolds, M. Warner, K. De Greve, Y. Dovzhenko, L. Thiel, R. L. Walsworth, S. Hong, P. Maletinsky, and A. Yacoby, Nat. Nanotechnol. **9**, 279 (2014).
[11]Y. Twig, E. Dikarov, and A. Blank, Mol. Phys. **111**(18–19), 2674 (2013).
[12]Y. Twig, E. Suhovoy, and A. Blank, Rev. Sci. Instrum. **81**(10), 104703 (2010).
[13]A. Blank and J. H. Freed, Isr. J. Chem. **46**(4), 423 (2006).
[14]R. Narkowicz, D. Suter, and I. Niemeyer, Rev. Sci. Instrum. **79**(8), 084702 (2008).
[15]A. Blank, C. R. Dunnam, P. P. Borbat, and J. H. Freed, J. Magn. Reson. **165**(1), 116 (2003).
[16]B. A. Abelan, M. Seelmann-Eggebert, D. Bruch, A. Leuther, H. Massler, B. Baldischweiler, M. Schlechtweg, J. D. Gallego-Puyol, I. Lopez-Fernandez, C. Diez-Gonzalez, I. Malo-Gomez, E. Villa, and E. Artal, IEEE Trans. Microwave Theory Tech. **60**(12), 4080 (2012).
[17]L. Alexander, K. N. Suwuntanasarn, and W. D. Hutchison, e-print arXiv:1009.4240v1 (2010).
[18]G. A. Rinard, R. W. Quine, R. T. Song, G. R. Eaton, and S. S. Eaton, J. Magn. Reson. **140**(1), 69 (1999).
[19]G. Feher, Phys. Rev. **114**, 1219 (1959).
[20]M. Steger, K. Saeedi, M. L. W. Thewalt, J. J. L. Morton, H. Riemann, N. V. Abrosimov, P. Becker, and H. J. Pohl, Science **336**(6086), 1280 (2012).
[21]R. Schirhagl, K. Chang, M. Loretz, and C. L. Degen, Annu. Rev. Phys. Chem. **65**, 83 (2014).
[22]J. J. L. Morton, D. R. McCamey, M. A. Eriksson, and S. A. Lyon, Nature **479**(7373), 345 (2011).
[23]V. Cerletti, W. A. Coish, O. Gywat, and D. Loss, Nanotechnology **16**(4), R27 (2005).
[24]Y. Twig, E. Dikarov, and A. Blank, J. Magn. Reson. **218**, 22 (2012).